

Bottomonium above deconfinement in lattice nonrelativistic QCD

G. Aarts^a, S. Kim^b, M. P. Lombardo^c, M. B. Oktay^d, S. M. Ryan^e, D. K. Sinclair^f and J.-I. Skullerud^g

^a*Department of Physics, Swansea University, Swansea SA2 8PP, United Kingdom*

^b*Department of Physics, Sejong University, Seoul 143-747, Korea*

^c*INFN-Laboratori Nazionali de Frascati, I-00044, Frascati (RM) Italy*

^d*Physics Department, University of Utah, Salt Lake City, Utah, USA*

^e*School of Mathematics, Trinity College, Dublin 2, Ireland*

^f*HEP Division, Argonne National Laboratory, 9700 South Cass Avenue, Argonne, Illinois 60439, USA*

^g*Department of Mathematical Physics, National University of Ireland Maynooth, Maynooth, County Kildare, Ireland*

(Dated: March 5, 2022)

We study the temperature dependence of bottomonium for temperatures in the range $0.4T_c < T < 2.1T_c$, using nonrelativistic dynamics for the bottom quark and full relativistic lattice QCD simulations for $N_f = 2$ light flavors on a highly anisotropic lattice. We find that the Υ is insensitive to the temperature in this range, while the χ_b propagators show a crossover from the exponential decay characterizing the hadronic phase to a power-law behaviour consistent with nearly-free dynamics at $T \simeq 2T_c$.

PACS numbers: 11.10.Wx, 12.38.Gc, 14.40.Pq

Introduction – Heavy quark bound states are important probes of the dynamics in the Quark Gluon Plasma: charmonium suppression [1, 2] has been observed at a variety of energies at SPS [3] and RHIC [4]. While the melting of bound states certainly reduces quarkonium production, the converse is not necessarily true: different, even competing, effects make it difficult to interpret charmonium suppression patterns. It has been noted that such effects should be less significant for bottomonium (see e.g. Ref. [5] for a review). Since at LHC energies bottomonium will be produced copiously [6, 7], precision studies of the suppression pattern and its unambiguous link with the spectrum of bound states should be possible. The advent of the LHC calls therefore for precision studies of bottomonium at high temperature.

Due to the large mass of the bottom quark, it is customary to study the bottomonium spectrum at zero temperature using nonrelativistic QCD (NRQCD) [8–10] and other effective field theories [11]. In this Letter, we employ NRQCD to study the response of bottomonium to a thermal medium of quarks and gluons in the temperature range $0.4T_c < T < 2.1T_c$, at the onset of the initial temperature attained in heavy ion collisions at the LHC [12]. We use dynamical anisotropic lattice configurations with two light flavors, which have been exploited before in a relativistic study of charmonium [13, 14]. As explained below, the use of NRQCD is a controlled approach which avoids many of the unwanted systematic effects encountered when using relativistic dynamics for bottomonium at nonzero temperature [15–17]. An early study of bottomonium at nonzero temperature using NRQCD (on a quenched background for the 1S_0 and 3S_1 states only) can be found in the pioneering work [18].

NRQCD at nonzero temperature – In contrast to the case at zero temperature [11], the use of potential models to analyse quarkonium at nonzero temperature is less well defined due to the uncertainty about which potential

to use (see e.g. Ref. [19] and references therein). Recently this has been clarified by casting the problem in the language of effective field theory at nonzero temperature [20–25]. The series of effective field theories that is obtained is based on the hierarchy $M \gg T > g^2M > gT \gg g^4M$, where M is the heavy quark mass and g is the gauge coupling. Ref. [26] provides a clear introduction. Integrating out thermal degrees of freedom generates an imaginary part for the interquark potential, which highlights the absence of stable states once they are immersed in a thermal medium. Limitations of approaches based on potential models and the Schrödinger equation are discussed in Ref. [27].

In the effective thermal field theory setup [20–26], NRQCD is the first theory obtained when integrating out ultraviolet degrees of freedom. We study this theory non-perturbatively on the lattice and therefore do not require weak-coupling arguments as in the hierarchy of effective field theories alluded to above. Since NRQCD relies on the scale separation $M \gg T$ and we study temperatures up to $2T_c \simeq 400$ MeV, its application is fully justified.

NRQCD has an additional advantage. At nonzero temperature, spectroscopy for relativistic quarks is hindered by the periodicity of the lattice in the temporal direction and the reflection symmetry of mesonic correlators, visible in, e.g., the standard relation between a correlation function and its spectral function,

$$G(\tau) = \int_0^\infty \frac{d\omega}{\pi} \frac{\cosh[\omega(\tau - 1/2T)]}{\sinh(\omega/2T)} \rho(\omega). \quad (1)$$

Nontrivial spectral weight at small ω yields a constant τ -independent contribution to the correlator, which must be treated with care [28, 29]. Moreover, it has been shown that this contribution can interfere with meson spectroscopy [30], which has cast doubt on the status of results for the melting or survival of charmonium at high temperature [30, 31].

In NRQCD these problems are not present. Writing $\omega = 2M + \omega'$ and dropping terms that are exponentially suppressed when $M \gg T$ [22], the spectral relation (1) reduces to

$$G(\tau) = \int_{-2M}^{\infty} \frac{d\omega'}{\pi} \exp(-\omega'\tau) \rho(\omega') \quad (\text{NRQCD}), \quad (2)$$

even at nonzero temperature. As a result, all problems associated with thermal boundary conditions are absent.

To study what to expect when quarks are no longer bound, consider free quarks in continuum NRQCD with energy $E_{\mathbf{p}} = \mathbf{p}^2/2M$. The correlators for the S and P waves are then of the form [22]

$$G_S(\tau) \sim \int \frac{d^3p}{(2\pi)^3} \exp(-2E_{\mathbf{p}}\tau) \sim \tau^{-3/2}, \quad (3)$$

$$G_P(\tau) \sim \int \frac{d^3p}{(2\pi)^3} \mathbf{p}^2 \exp(-2E_{\mathbf{p}}\tau) \sim \tau^{-5/2}, \quad (4)$$

i.e., they decay as a power for large euclidean time. Of course, interactions and finite lattice spacing and volume effects are expected to modify this in the realistic case.

Lattice simulations – Gauge configurations with two degenerate dynamical light Wilson-type quark flavors are produced on highly anisotropic lattices ($\xi \equiv a_s/a_\tau = 6$) of size $N_s^3 \times N_\tau$. A summary of the lattice datasets is given in Table I, while more details of the lattice action and parameters can be found in Refs. [13, 14]. We computed NRQCD propagators on these configurations using a mean-field improved action with tree-level coefficients, which includes terms up to and including $\mathcal{O}(v^4)$, where v is the typical velocity of a bottom quark in bottomonium (see Ref. [32] for a discussion of the systematics). The states we consider are listed in Table II.

An accurate determination of bottomonium spectroscopy requires careful tuning of the bare heavy quark mass m_b to satisfy NRQCD dispersion relations [9]. Since the main goal of this work is to study the finite-temperature modification of NRQCD propagators, an approximate choice of $a_s m_b$ is made such that $m_b \simeq 5$ GeV.

Zero temperature results – The zero temperature spectrum from our analysis is summarized in Table II. This spectrum is obtained using a combination of point and extended sources in the different channels, in order to extract both the ground state and the first excited state.

N_s	N_τ	a_τ^{-1}	$T(\text{MeV})$	T/T_c	No. of Conf.
12	80	7.35GeV	90	0.42	74
12	32	7.06GeV	221	1.05	500
12	24	7.06GeV	294	1.40	500
12	16	7.06GeV	441	2.09	500

TABLE I: Summary of the lattice data set. The lattice spacing is set using the $1P - 1S$ spin-averaged splitting in charmonium [33].

state	$a_\tau \Delta E$	Mass (MeV)	Exp. (MeV) [34]
$1^1S_0(\eta_b)$	0.118(1)	9438(7)	9390.9(2.8)
$2^1S_0(\eta_b(2S))$	0.197(2)	10009(14)	-
$1^3S_1(\Upsilon)$	0.121(1)	9460*	9460.30(26)
$2^3S_1(\Upsilon')$	0.198(2)	10017(14)	10023.26(31)
$1^1P_1(h_b)$	0.178(2)	9872(14)	-
$1^3P_0(\chi_{b0})$	0.175(4)	9850(28)	9859.44(42)(31)
$1^3P_1(\chi_{b1})$	0.176(3)	9858(21)	9892.78(26)(31)
$1^3P_2(\chi_{b2})$	0.182(3)	9901(21)	9912.21(26)(31)

TABLE II: Zero temperature bottomonium spectroscopy from NRQCD. The $1^3S_1(\Upsilon)$ state is used to set the scale.

Because level splittings are relatively insensitive to m_b and to avoid the difficulties in calculating the rest mass in NRQCD, we have combined $m_\Upsilon(1^3S_1) = 9460$ MeV (from the Particle Data Book [34]) with the mass splittings obtained from our results to predict the bottomonium spectrum.

As can be seen from Table II, the zero temperature spectrum is reproduced reasonably well. The hyperfine splitting between the $\eta_b(1^1S_0)$ and $\Upsilon(1^3S_1)$ is much smaller than the experimental value, due to the coarse spatial lattice spacing, the use of tree-level coefficients, the relatively heavy sea quarks and contributions of higher order in v^2 (see Ref. [32] for earlier calculations and discussions). In this study we are primarily interested in qualitative changes to the Υ and χ_b correlators as the temperature changes, so a precision determination is not a major concern.

Υ and χ_b in the plasma – To investigate thermal effects, we focus on the Υ and χ_b states, computed with point sources. Following the discussion above, our aim is to see a transition from exponential decay in the hadronic phase, $G(\tau) \sim \exp(-\Delta E\tau)$, characterizing bound states, to power law decay, $G(\tau) \sim \tau^{-\gamma}$, see Eqs. (3, 4), characterizing quasi-free behaviour.

In Fig. 1, standard effective masses, defined by

$$m_{\text{eff}}(\tau) = -\log[G(\tau)/G(\tau - a_\tau)], \quad (5)$$

are shown for both the Υ and the χ_{b1} propagators at various temperatures. Single exponential decay should yield a τ -independent plateau. In both cases we find that at the lowest temperature, $T = 0.42T_c$, exponential behaviour is visible provided one goes to late euclidean times. Relevant for the topic of this Letter is that in the case of the Υ , the data at the higher temperatures do not show any significant deviation from the low-temperature result. On the other hand for the χ_{b1} a strong temperature dependence is visible, especially at the two highest temperatures, ruling out pure exponential long time decay. We take this as a first indication that the Υ is not sensitive to the quark-gluon plasma up to $T \simeq 2T_c$, while the χ_b may melt at much lower temperatures.

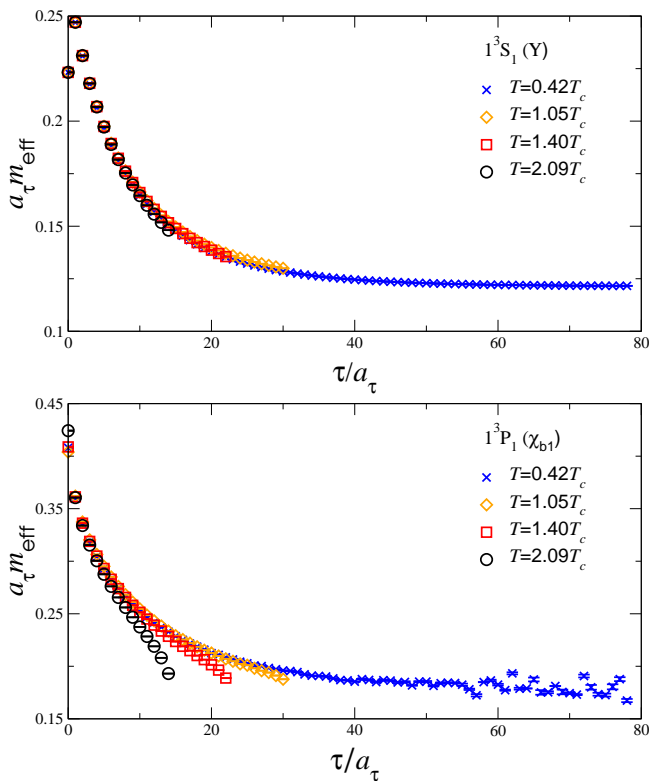


FIG. 1: Effective mass plots for the Υ (above) and χ_{b1} (below) using point sources for various temperatures: note the different temperature dependence.

To investigate the behavior of the χ_b propagators in more detail, we display in Fig. 2 the χ_{b0} , χ_{b1} and χ_{b2} propagators on a log-log scale, at the highest temperature $T = 2.09T_c$. The straight line is a fit of the form $G(\tau) = c\tau^{-d}$, which is motivated by the continuum expression in the absence of interactions (4). We conclude that a power decay describes the data well at large euclidean time, with a power $d = 2.605(1)$ which is close to the continuum noninteracting value of $5/2$.

To visualize the approach to quasi-free behaviour in another way, we construct effective power plots, using the definition

$$\gamma_{\text{eff}}(\tau) = -\tau \frac{G'(\tau)}{G(\tau)} = -\tau \frac{G(\tau + a_\tau) - G(\tau - a_\tau)}{2a_\tau G(\tau)}, \quad (6)$$

where the prime denotes the (discretized) derivative. For a power decay, $G(\tau) \sim \tau^{-\gamma}$, this yields a constant result, $\gamma_{\text{eff}}(\tau) = \gamma$. On the other hand, for an exponential decay, $G(\tau) \sim \exp(-\Delta E\tau)$, this yields a linearly rising result, $\gamma_{\text{eff}}(\tau) = \Delta E\tau$. The results are shown in Fig. 3. We confirm again that the Υ displays essentially no temperature dependence, while for the χ_{b1} we observe a tendency to flatten out, corresponding to power decay at large euclidean time. Also shown are the effective exponents in the continuum noninteracting limit. In the case of the χ_{b1} , we observe that the effective exponent tends towards

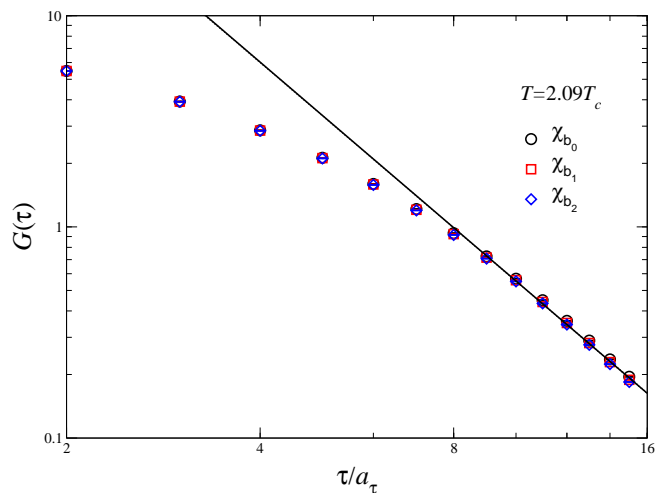


FIG. 2: χ_b propagators on a log-log scale, at the highest temperature $T = 2.09T_c$. The straight line is a fit to $G(\tau) = c\tau^{-d}$, with $c = 223.2 \pm 0.5$ and $d = 2.605 \pm 0.001$, using $\tau/a_\tau = 10, \dots, 15$.

the noninteracting result at the highest temperature we consider.

Summary – We have studied the behavior of Υ and χ_b at high temperature using anisotropic lattice simulations. The bottom quark is treated via NRQCD and the light quark dynamics is realized by exploiting lattice configurations with two flavors of dynamical quarks. The non-relativistic approximation for the bottom quark is well justified in the range of temperatures we have explored, and has many technical advantages. At nonzero temperature, the main benefit of using NRQCD over the standard relativistic formulation is that the only temperature dependence in the NRQCD correlators is due to the thermal medium, and not due to thermal boundary conditions. We found that this offers a much cleaner signal for the crossover between bound and melted states. It also improves the prospects for extracting spectral functions inverting Eq. (2) using the Maximal Entropy Method. This is currently in progress. It will also be interesting to compare the results presented here with those obtained using a relativistic treatment of bottom quarks, employing the same anisotropic action as was used for charmonium [13, 33]. This will give an estimate of the possible systematic uncertainties inherent in the two formulations.

Our results indicate that the Υ shows no temperature dependence up to $2.09T_c$, while the χ_b propagators are sensitive to the presence of the thermal medium immediately above T_c . Power-law decay of the χ_b propagators is visible at $T = 1.4T_c$, while at the highest temperature studied, $T \simeq 2T_c$, we found consistency with nearly-free dynamics. The effective power, defined in Eq. (6), is temperature dependent and approaches the noninteracting result at the highest temperature we considered. It

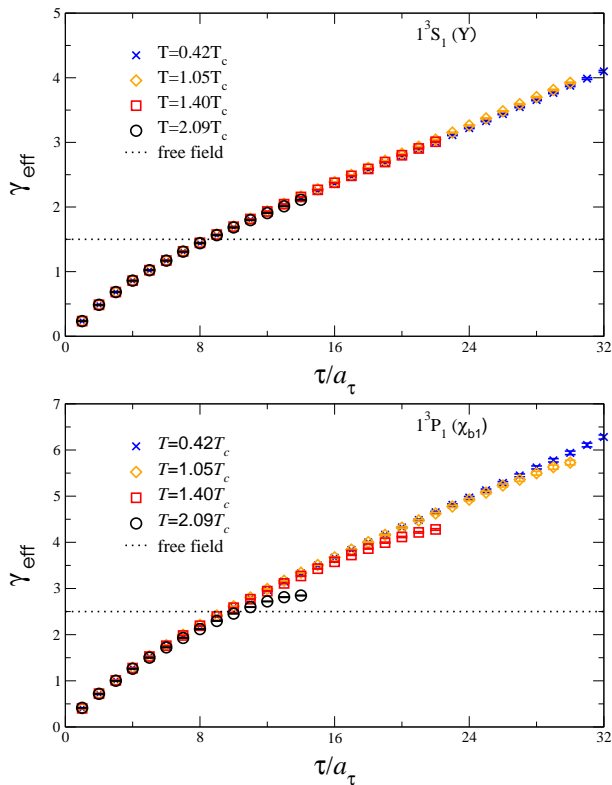


FIG. 3: Effective exponents $\gamma_{\text{eff}}(\tau)$ for the Υ (above) and χ_{b1} (below), as a function of Euclidean time for various temperatures. The dotted line indicates the noninteracting result in the continuum.

would be interesting to understand the temperature dependence and crossover between exponential and power decay analytically, within the framework of effective field theories mentioned above.

MPL thanks Helmut Satz, Peter Petreczky and participants in the “In Media” group of the Quarkonium Working Group for fruitful discussions. SK and MPL thank the Yukawa Institute of Theoretical Physics, Kyoto, and GA and MPL thank Trinity College Dublin and the National University of Ireland Maynooth, for their hospitality. SMR and JIS are grateful to the Trinity Centre for High-Performance Computing for their support. GA is supported by STFC. SK is supported by the National Research Foundation of Korea grant funded by the Korea government (MEST) No. 2010-0022219. DKS is supported in part by US Department of Energy contract DE-AC02-06CH11357. JIS is supported by Science Foundation Ireland grant 08-RFP-PHY1462. SMR is supported by the Research Executive Agency (REA) of the European Union under Grant Agreement number PITN-GA-2009-238353 (ITN STRONGnet).

- [1] T. Matsui and H. Satz, Phys. Lett. B **178** (1986) 416.
- [2] H. Satz, Nucl. Phys. A **783** (2007) 249.
- [3] R. Arnaldi [NA60 Collaboration], Nucl. Phys. A **830** (2009) 345C.
- [4] A. Adare *et al.* [PHENIX Collaboration], Phys. Rev. Lett. **101** (2008) 122301.
- [5] R. Rapp, D. Blaschke and P. Crochet, arXiv:0807.2470 [hep-ph].
- [6] B. Alessandro *et al.* [ALICE Collaboration], J. Phys. G **32** (2006) 1295.
- [7] J. P. Lansberg *et al.*, AIP Conf. Proc. **1038** (2008) 15.
- [8] G. P. Lepage *et al.*, Phys. Rev. D **46** (1992) 4052.
- [9] C. T. H. Davies *et al.*, Phys. Rev. D **50** (1994) 6963.
- [10] G. T. Bodwin, E. Braaten and G. P. Lepage, Phys. Rev. D **51** (1995) 1125 [Erratum-ibid. D **55** (1997) 5853].
- [11] N. Brambilla, A. Pineda, J. Soto and A. Vairo, Rev. Mod. Phys. **77** (2005) 1423.
- [12] U. A. Wiedemann, Nucl. Phys. A **830** (2009) 74C.
- [13] G. Aarts, C. Allton, M. B. Oktay, M. Peardon and J. I. Skullerud, Phys. Rev. D **76** (2007) 094513.
- [14] R. Morrin, A. O. Cais, M. Peardon, S. M. Ryan and J. I. Skullerud, Phys. Rev. D **74** (2006) 014505.
- [15] A. Jakovac, P. Petreczky, K. Petrov and A. Velytsky, Phys. Rev. D **75** (2007) 014506.
- [16] P. Petreczky, J. Phys. G **37** (2010) 094009.
- [17] R. Rapp and H. van Hees, arXiv:0903.1096 [hep-ph].
- [18] J. Fingberg, Phys. Lett. B **424** (1998) 343.
- [19] A. Mocsy and P. Petreczky, Phys. Rev. D **77** (2008) 014501.
- [20] M. Laine, O. Philipsen, P. Romatschke and M. Tassler, JHEP **0703** (2007) 054.
- [21] M. Laine, JHEP **0705** (2007) 028.
- [22] Y. Burnier, M. Laine and M. Vepsalainen, JHEP **0801** (2008) 043.
- [23] A. Beraudo, J. P. Blaizot and C. Ratti, Nucl. Phys. A **806** (2008) 312.
- [24] N. Brambilla, J. Ghiglieri, A. Vairo and P. Petreczky, Phys. Rev. D **78** (2008) 014017.
- [25] N. Brambilla, M. A. Escobedo, J. Ghiglieri, J. Soto and A. Vairo, arXiv:1007.4156 [hep-ph].
- [26] M. Laine, Nucl. Phys. A **820** (2009) 25C.
- [27] A. Beraudo, J. P. Blaizot, P. Faccioli and G. Garberoglio, Nucl. Phys. A **846** (2010) 104.
- [28] G. Aarts and J. M. Martinez Resco, JHEP **0204** (2002) 053.
- [29] G. Aarts, C. Allton, J. Foley, S. Hands and S. Kim, Phys. Rev. Lett. **99** (2007) 022002.
- [30] T. Umeda, Phys. Rev. D **75** (2007) 094502.
- [31] P. Petreczky, Eur. Phys. J. C **62** (2009) 85.
- [32] C. T. H. Davies *et al.* [UKQCD Collaboration], Phys. Rev. D **58** (1998) 054505.
- [33] M. B. Oktay and J. I. Skullerud, arXiv:1005.1209 [hep-lat].
- [34] K. Nakamura [Particle Data Group], J. Phys. G **37** (2010) 075021.